LEVEL SET SEGMENTATION OF DERMOSCOPY IMAGES

Margarida Silveira, Jorge S. Marques

Instituto Superior Técnico
Instituto de Sistemas e Robótica

ABSTRACT

This paper presents a method for the segmentation of skin lesions in dermoscopy images. The proposed technique uses region based level sets and adopts a mixture of Gaussian densities as the probabilistic model for both the lesion and the skin regions. The Estimation-Maximization (EM) algorithm is used to estimate the probability density functions in each region. Experimental results which demonstrate the effectiveness of the proposed technique are presented.

***Index Terms*—** dermoscopy, segmentation, level sets, EM-algorithm

1. INTRODUCTION

Dermoscopy is a non-invasive diagnostic technique for the in vivo observation of pigmented skin lesions used in dermatology [1]. Dermoscopy images have great potential in the early diagnostic of malignant melanoma, which is a type of skin cancer, but their interpretation is time consuming and subjective, even for trained dermatologists. Therefore, there is currently a great interest in the development of computer-aided diagnostic systems that can assist the clinical diagnosis of dermatologists. One of the most important steps of such a system is the segmentation of the lesion boundary, and one that affects the accuracy of subsequent feature extraction steps. However, segmentation is difficult because of the wide range of lesion shapes, sizes and colors and also different skin tones (see Figure 1). In addition, some lesions have irregular boundaries and in some cases there is a smooth transition between the lesion and the skin. Another difficulty is the presence of dark hair covering the lesions.

To address this problem several algorithms have been proposed. For instance in [2] a fusion of global thresholding, adaptive thresholding and clustering is used, in [3] the segmentation is based on the zero-crossings of the Laplacian-of-Gaussian, [4] uses multi-scale region growing, [5] proposes a modified fuzzy c-means algorithm which is orientation sensitive and [7] proposes statistical region merging. Active contours, both parametric and geometric, have also been proposed for the segmentation of skin lesions. In [6] the geodesic gradient vector flow (GVF) is used, in [8] two approaches are used: the geodesic active contours model and the geodesic edge tracing. Active contours based on edges require the initialization to be close to the final boundary and are sensitive to noise and weak edges. To address these difficulties two approaches are proposed in [9], a robust edge based parametric active contour and a region based geometric method.

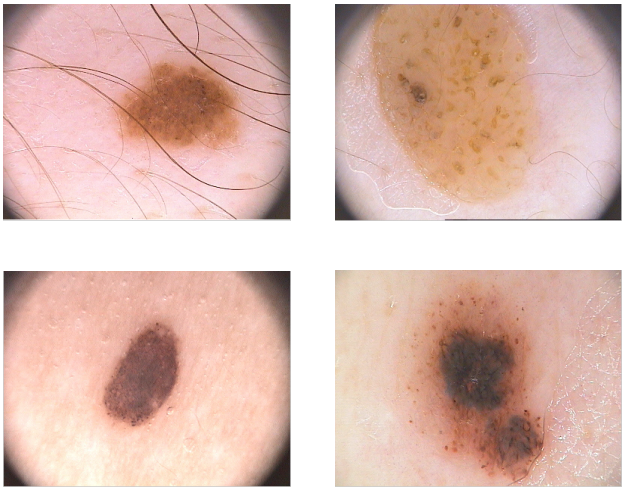

Fig. 1. The diversity of dermoscopy images.

The method proposed is this paper is also a region based geometric method but includes a major contribution: it uses a different probabilistic model for the regions which allows better region characterization and leads to more precise boundaries. This will be shown by experimental results.

The remainder of this paper is organized as follows: section 2 describes the proposed method for level set segmentation, section 3 describes the experimental results and section 4 concludes the paper.

2. LEVEL SET SEGMENTATION

In this work we assume that the image is formed by two regions Ω_1 and Ω_2 separated by a curve C, and that regions Ω_1 and Ω_2 are modeled by probability density functions p_1 and p_2, respectively. The segmentation is obtained by minimizing the following energy function [10]:

$$E(C, p_1, p_2) = \mu lenght(C) + \lambda_1 \int_{\Omega_1} \log p_1 dx + \lambda_2 \int_{\Omega_2} \log p_2 dx \quad (1)$$

In this equation the first term is a regularizing term that depends on the length of the curve and μ, λ_1 and λ_2 are positive weighting parameters.

Using the level set formulation [12], embedding the curve C as the zero level set $C(t) = \{(\vec{x})|\phi(t, \vec{x}) = 0\}$ of a higher dimensional level set function $\Phi(t, \vec{x})$ this energy function can be rewritten as:

$$\begin{aligned} E(\Phi, p_1, p_2) &= \mu \int_{\Omega} \delta(\Phi) \left|\nabla\Phi\right| dx \\ &- \int_{\Omega} \left[H(\Phi) \log p_1 + (1 - H(\Phi)) \log p_2\right] dx \end{aligned} \quad (2)$$

where H is the Heaviside function, $H(z) = 1$ for $z \geq 0$ and $H(z) = 0$ for $z < 0$. The evolution of Φ is governed by the following motion Partial Differential Equation (PDE):

$$\frac{\partial\Phi}{\partial t} = \delta_\varepsilon(\Phi) \left[\begin{array}{l} \mu div\left(\frac{\nabla\Phi}{|\nabla\Phi|}\right) - \lambda_1 \log p_1(y|\hat{\theta}_1) + \\ \lambda_2 \log p_2(y|\hat{\theta}_2) \end{array} \right] \quad (3)$$

where $\delta_\varepsilon(\Phi)$ is a regularized version of the dirac delta function.

Usually, the regions are modeled by single Gaussian densities which leads to:

$$\log p_i = C_0 - \frac{1}{2}(I - \mu_i)^T R^{-1}(I - \mu_i) \quad (4)$$

where C_0 is a constant. Assuming that the covariance matrix is the same for both regions and satisfies $R = \sigma^2 I_n$ where $I_n \in \mathbb{R}^{n \times n}$ is the identity matrix of dimension $n \times n$, we get the model adopted in [10]:

$$\log p_i = C_0 - C_1 \left\|I - \mu_i\right\|^2 \quad (5)$$

However, this model is too restrictive, it is unable to represent the different colors which are usually present in both the lesions and the skin. Therefore, in this work we adopted a more flexible model to represent these regions which is the mixture of Gaussians model:

$$p(y|\theta) = \sum_{m=1}^{K} \alpha_m p(y|\theta_m) \quad (6)$$

where K is the number of components, $\alpha_1 ... \alpha_K$ are the mixing probabilities summing to one and each θ_m is the set of parameters of the m^{th} component. Since we assume Gaussian components we have $\theta_m = [\mu_m, R_m]$.

At every iteration of the level set method the mixture of Gaussians is estimated with the EM algorithm [13]. The EM algorithm alternates between two steps. In the E-step, a set of weights summing to one is assigned to each region point y^j, $j = 1, ..., N$, where y^j has 3 components, corresponding to the RGB color channels:

$$w_k^j = \frac{\alpha_k p(y^j|\hat{\theta}_k)}{\sum_{m=1}^{K} \alpha_m p(y^j|\hat{\theta}_m)} \quad (7)$$

and in the M-step the parameters of each component are updated:

$$\mu_k = \frac{\sum_{j=1}^{N} w_j^k y^j}{\sum_{j=1}^{N} w_j^k} \quad (8)$$

$$R_k = \frac{\sum_{j=1}^{N} w_j^k (y^j - \mu_k)(y^j - \mu_k)^T}{\sum_{j=1}^{N} w_j^k} \quad (9)$$

and the mixing proportions are updated by:

$$\alpha_k = \frac{1}{N} \sum_{j=1}^{N} w_j^k \quad (10)$$

Experimentally, we found that 3 components was enough for the lesions regions and 2 components for the skin.

2.1. Preprocessing and initialization

The images were filtered with the morphological closing filter using a disk as structuring element in order to remove the features from dark hair and additionally with a median filter. Then, the dark regions in the 4 corners of the images were removed by gray-level thresholding using Otsu's method [11] followed by elimination of the components that were connected to each of the four corners.

To initialize the contour the user selects a rectangular region in the lesion region. The initialization doesn't have to be very close to the final boundary, it doesn't have to be totally inside or outside the lesion, but it is important that the significant lesion colors are represented in the initial contour.

3. EXPERIMENTAL RESULTS

The method was tested on a set of 50 dermoscopy color images from Hospital Pedro Hispano. These are color images (RBG) with 24-bits per pixel and 764 x574 pixels of spatial resolution. The segmentation results were compared with those of the level set algorithm of [10], using manually obtained contours as the ground truth. These ground truth contours were obtained by a non specialist but they were considered the best among a variety of methods by an experienced dermatologist [9]. The level set algorithm described

in [10] models the regions by single Gaussian densities with fixed standard deviation (eq. 5) and will be denoted (SG-LS) as opposed to mixture of Gaussians level sets (MG-LS). Two different metrics suggested in [14] were used to quantify the boundary differences; the Hammoude distance which is based on a pixel by pixel comparison of the pixels enclosed by the two boundaries and the Hausdorf distance which finds the largest distance between the boundary points. Let X and Y denote the two binary images such that all the pixels inside the curve have label 1 and all the others have label 0. The Hammoude distance is calculated by:

$$dHamm(X,Y) = \frac{\#(X \cup Y) - \#(X \cap Y)}{\#(X \cup Y)} \quad (11)$$

Let $A = \{a_1, a_2, ...a_m\}$ and $B = \{b_1, b_2, ...b_n\}$ denote the set of points belonging to contour A and contour B respectively. The distance from a_i to its closest point (DCP) in B is given by:

$$d(a_i, B) = \min_j \|b_j - a_i\| \quad (12)$$

The Hausdorf distance is the maximum of the distance to the closest points between the two curves:

$$dHaus(A,B) = \max\{\max_i d(a_i, B), \max_j d(b_j, A)\} \quad (13)$$

Results of the Hammoude and Hausdorf distances calculated for the 50 images are presented in Table 1.

	Hammoude		Hausdorf	
	Mean	Var	Mean	Var
MG-LS	0.147	0.008	22.05	341
SG-LS	0.192	0.011	33.65	1258

Table 1. Hammoude and Hausdorf distances between obtained contours and manual contours

Both metrics illustrate that the proposed method is better than the SG-LS method. The differences between the two methods are statistically significant since both metrics obtained $p < 0.05$ using a paired t-test. Some examples are presented in Figure 2 where the final contour is superimposed in red. The segmentation results are good even in the presence of hair or when the lesion or the skin has different colors.

For the images that have good contrast between the lesion and the skin, the result of both methods is very similar. However, in cases where there is a smooth transition between the lesion and the skin, the proposed method is clearly superior. Examples of this are shown in Figure 3, where the segmentation results of both methods are presented for comparison.

Figure 4 compares the histogram of intensity values in the lesion regions with the pdf's estimated with the EM algorithm for the three color channels of the RGB image from figure 2 (b). The histogram is shown in blue and the pdf is shown in red. It can be seen that the two curves are very close thus the estimated pdf is a good approximation.

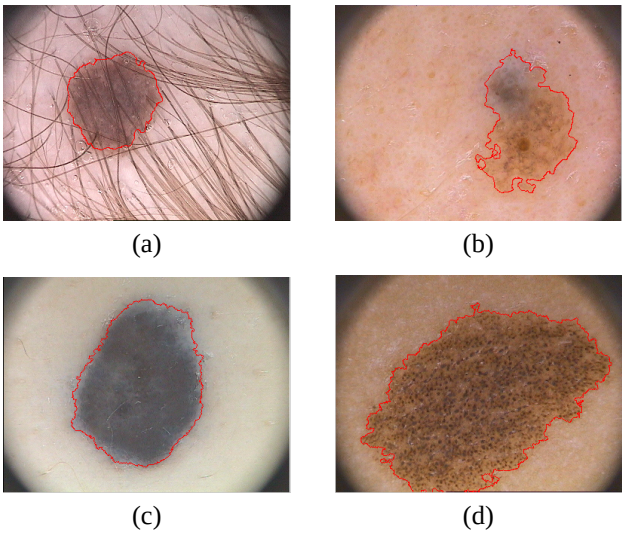

Fig. 2. Segmentation results.

4. ACKNOWLEDGMENTS

This work was supported by Fundação para a Ciência e a Tecnologia (ISR/IST plurianual funding) through the POS Conhecimento Program that includes FEDER funds. This work was performed in the scope of collaborations with Profs. Teresa Mendonça and André Marçal from the University of Porto. The authors would like to thank Dr. Jorge Rozeira and Hospital Pedro Hispano for providing the images.

5. CONCLUSIONS

In this paper we propose a method for the segmentation of skin lesions in dermoscopy images based on the level set framework and using a mixture of Gaussian densities as the probabilistic model for both the lesion and the skin regions. The segmentation is based on the level set framework and the EM algorithm is used to estimate the probability density functions in each region. The segmentation results were compared with those of the level set method using single Gaussian densities with fixed standard deviation, using manually obtained contours as the ground truth and obtained better results. Future work includes the automatic estimation of the number of mixture components.

6. REFERENCES

[1] Argenziano, G., Soyer, H. P., De Giorgi, V., et al., Dermoscopy, an interactive atlas. Milan, Italy: EDRA Medical

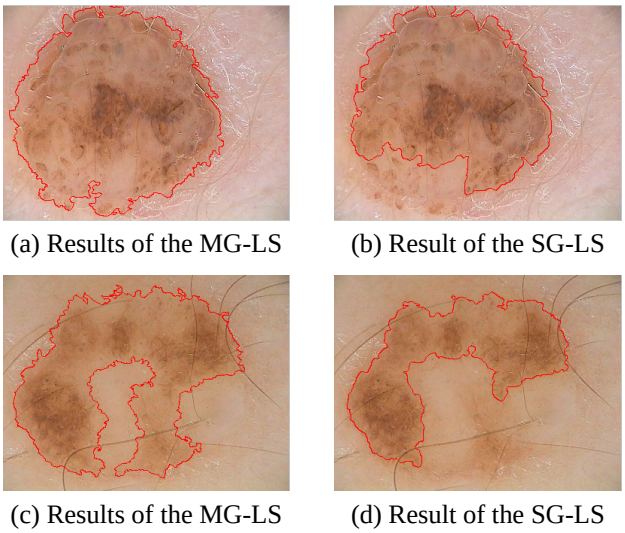

(a) Results of the MG-LS (b) Result of the SG-LS

(c) Results of the MG-LS (d) Result of the SG-LS

Fig. 3. Segmentation results of both methods when the transition between the lesion and the skin is smooth.

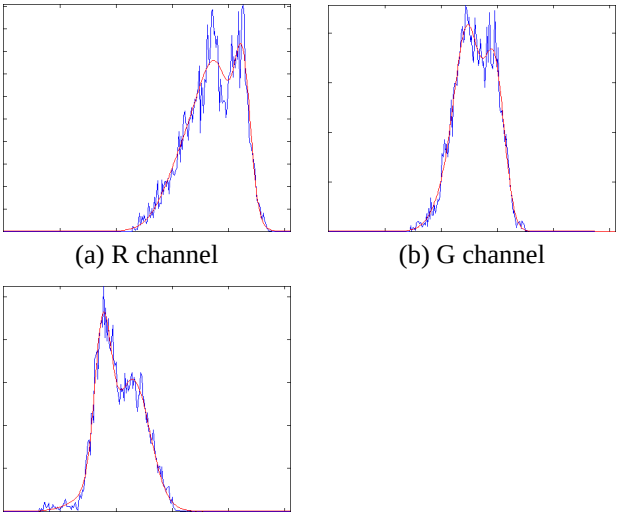

(a) R channel (b) G channel

(c) B channel

Fig. 4. Comparison between histogram and estimated pdf in the lesion region.

Publishing. (http://www.dermoscopy.org), 2000.

[2] Ganster, H.; Pinz, P.; Rohrer, R.; Wildling, E.; Binder, M.; Kittler, H., Automated melanoma recognition. IEEE Transactions on Medical Imaging, vol.20, no.3, pp. 233-239, Mar 2001.

[3] Rubegni, P.; Ferrari, A.; Cevenini, G.; Piccolo, D.; Burroni, M.; Perotti, R.; Peris, K.; Taddeucci, P.; Biagioli, M.; Dell'Eva, G.; Chimenti, S.; Andreassi, L., Differentiation between pigmented Spitz naevus and melanoma by digital dermoscopy and stepwise logistic discriminant analysis. Melanoma Research. vol. 11, no.1: pp. 37-44, February 2001.

[4] Celebi, M. E.; Aslandogan, Y. A.; Bergstresser, P. R., Unsupervised border detection of skin lesion images. International Conference on Information Technology: Coding and Computing, ITCC 2005, vol.2, no., pp. 123-128, 4-6 April 2005.

[5] Schmid-Saugeona P., Guillodb J., Thirana J. P., Towards a computer-aided diagnosis system for pigmented skin lesions. Computerized Medical Imaging and Graphics, vol. 27, pp. 65-78, 2003.

[6] Erkol, B., Moss, R. H., Stanley, R. J., Stoecker, W. V. and Hva-tum, E., Automatic lesion boundary detection in dermoscopy images using gradient vector flow snakes. Skin Research & Technology, vol. 11, pp. 17-26, 2005.

[7] Celebi, M., Kingravi, H., Lee, J., Fast and Accurate Border Detection in Dermoscopy Images Using Statistical Region Merging. Proceeding of SPIE Medical Imaging, Feb. 17 - 22. San Diego, CA, USA, 2007.

[8] Do Hyun Chung; Sapiro, G., Segmenting skin lesions with partial-differential-equations-based image processing algorithms. IEEE Transactions on Medical Imaging, vol. 19, no.7, pp. 763-767, Jul 2000.

[9] Mendonca, T., Marcal, A., Vieira, A., Nascimento, J., Silveira, M., Marques, J., Rozeira, J., Comparison of Segmentation Methods for Automatic Diagnosis of Dermoscopy Images. IEEE International Conference in Medicine and Biology Society, EMBS 2007, vol., no., pp. 6572-6575, 22-26 Aug. 2007.

[10] T. E. Chan, B.Y. Sandberg,L.A. Vese, Active contours without edges for vector-valued images, Journal of Visual Communications and Image Representation, vol.11, pp. 130-141, 2000.

[11] Otsu, N.: A threshold selection method from gray-level histograms. IEEE Transactions on Systems, Man and Cybernetics, SMC-9, pp. 62-66, 1979.

[12] Osher, S. and Sethian, J., Fronts propagating with curvature-dependent speed: Algorithms based on Hamilton-Jacobi equations. Jour. Comp. Phys, 79:12-49, 1988.

[13] McLachlan, G. and Krishnan, T., The EM Algorithm and Extensions, John Wiley & Sons, New York, 1997.

[14] Chalana,V. and Kim, Y., A methodology for evaluation of boundary detection algorithms on medical images. IEEE Transactions on Medical Imaging, vol. 16, no. 5, pp. 642-652, 1997.